

QGIS-Based Tools to Evaluate Air Flow Rate by Natural Ventilation in Buildings at Urban Scale

Original

QGIS-Based Tools to Evaluate Air Flow Rate by Natural Ventilation in Buildings at Urban Scale / Santantonio, Silvia; Mutani, Guglielmina. - ELETTRONICO. - Building Simulation Applications BSA 2022:(2023), pp. 331-339. (Intervento presentato al convegno 5 IBPSA-ITALY CONFERENCE tenutosi a Bolzano nel June-July 2022) [10.13124/9788860461919].

Availability:

This version is available at: 11583/2977557 since: 2023-03-28T19:14:43Z

Publisher:

BU Press

Published

DOI:10.13124/9788860461919

Terms of use:

openAccess

This article is made available under terms and conditions as specified in the corresponding bibliographic description in the repository

Publisher copyright

(Article begins on next page)

unibz —
Freie Universität Bozen
Libera Università di Bolzano
Università Lìdia de Bulsan

Konferenzbeiträge / Atti / Proceedings

Building Simulation Applications BSA 2022

5th IBPSA-Italy Conference
Bozen-Bolzano, 29th June –1st July 2022

Edited by

**Giovanni Pernigotto, Francesco Patuzzi,
Alessandro Prada, Vincenzo Corrado, Andrea Gasparella**

bu,press

bozen
bolzano
university
press

Scientific Committee

Ian Beausoleil-Morrison, Carleton University, Canada
Jan L.M. Hensen, Technische Universiteit Eindhoven, The Netherlands
Gregor P. Henze, University of Colorado Boulder, USA
Ardeshir Mahdavi, Technische Universität Wien, Austria
Athanasios Tzempelikos, Purdue University, USA
Reinhard Radermacher, University of Maryland, USA
Francesco Asdrubali, Università degli Studi Roma Tre, Italy
Paolo Baggio, Università degli Studi di Trento, Italy
Francesca Cappelletti, Università IUAV di Venezia, Italy
Maurizio Cellura, Università degli Studi di Palermo, Italy
Cristina Cornaro, Università degli Studi di Tor Vergata, Italy
Vincenzo Corrado, Politecnico di Torino, Italy
Andrea Gasparella, Free University of Bozen-Bolzano, Italy
Livio Mazzarella, Politecnico di Milano, Italy
Adolfo Palombo, Università degli Studi di Napoli Federico II, Italy

Students Tutoring Scientific Committee

Matthias Schuss, Technische Universität Wien, Austria
Ulrich Pont, Technische Universität Wien, Austria
Alessia Arteconi, Università Politecnica delle Marche, Italy
Ilaria Ballarini, Politecnico di Torino, Italy
Annamaria Buonomano, Università degli Studi di Napoli Federico II, Italy
Marco Caniato, Free University of Bozen-Bolzano, Italy
Gianpiero Evola, Università degli Studi di Catania, Italy
Federica Morandi, Free University of Bozen-Bolzano, Italy
Francesco Patuzzi, Free University of Bozen-Bolzano, Italy
Giovanni Pernigotto, Free University of Bozen-Bolzano, Italy
Anna Laura Pisello, Università degli Studi di Perugia, Italy
Alessandro Prada, Università degli Studi di Trento, Italy

Organizing Committee

Paolo Baggio, Università degli Studi di Trento, Italy
Marco Baratieri, Free University of Bozen-Bolzano, Italy
Marco Caniato, Free University of Bozen-Bolzano, Italy
Francesca Cappelletti, Università IUAV di Venezia, Italy
Vincenzo Corrado, Politecnico di Torino, Italy
Andrea Gasparella, Free University of Bozen-Bolzano, Italy
Norbert Klammsteiner, Energytech G.m.b.H./S.r.l -Bozen, Italy
Federica Morandi, Free University of Bozen-Bolzano, Italy
Francesco Patuzzi, Free University of Bozen-Bolzano, Italy
Giovanni Pernigotto, Free University of Bozen-Bolzano, Italy
Alessandro Prada, Università degli Studi di Trento, Italy
Fabio Viero, Manens – Tifs, Italy

bu,press

Bozen-Bolzano University Press, 2022

Free University of Bozen-Bolzano

www.unibz.it/universitypress

Cover design: DOC.bz / bu,press

ISSN 2531-6702

ISBN 978-88-6046-191-9

DOI 10.13124/9788860461919



This work—excluding the cover and the quotations—is licensed under the Creative Commons Attribution-ShareAlike 4.0 International License.

Table of Contents

Preface	ix
Optimization of Daylighting and Energy Performance in Bangladesh Ready-Made Garment Factories: Use of Parametric Design, Simulation Modeling, and Genetic Algorithms <i>Md Ashikur Rahman Joarder, Md Monir Hossain, Aaron J.E. Bach, Jean P. Palutikof, Fahim Tonmoy</i>	1
Transient Three-Dimensional CFD Modelling of Ceiling Fans: A Comparison Between Detailed and Simplified Models <i>Francesco Babich, Akshit Gupta, Wilmer Pasut</i>	9
Intelligibility Prediction in Scholar Classrooms <i>Samantha Di Loreto, Fabio Serpilli, Valter Lori, Costanzo Di Perna</i>	17
Hybrid Heat Pump Systems: Is Predictive Control Worth Using? <i>Patricia Ercoli, Alice Mugnini, Fabio Polonara, Alessia Arteconi</i>	25
The Acoustic Adaptation of the Aula Magna at the University of Bologna: Auditorium and Conference Hall Scenarios Simulated in the Main Nave of Santa Lucia's Church <i>Antonella Bevilacqua, Ruoran Yan, Maria Cristina Tommasino</i>	33
Implementation and Calibration of a Model to Treat Naturally Ventilated Complex Fenestration Systems in TRNSYS <i>Ingrid Demanega, Giovanni Gennaro, Giuseppe De Michele, Francesco Isaia, Fabio Favoino, Stefano Avesani</i>	41
Heat and Mass Transfer Modelling for Moisture-Related Risks in Walls Retrofitted by Timber Materials <i>Gianpiero Evola, Alessandra Urso, Vincenzo Costanzo, Francesco Nocera, Luigi Marletta</i>	49
Multi-Objective Optimization Of Thermo-Acoustic Comfort Of School Buildings <i>Daniele Colarossi, Samantha Di Loreto, Eleonora Tagliolini, Paolo Principi, Fabio Serpilli</i>	67
A Review on the FIVA-Project: Simulation-Assisted Development of Highly-Insulating Vacuum Glass Windows <i>Ulrich Pont, Peter Schober, Magdalena Wölzl, Matthias Schuss, Jakob Haberl</i>	69
Influence of Sound-Absorbing Ceiling on the Reverberation Time. Comparison Between Software and Calculation Method EN 12354-6 <i>Nicola Granzotto, Paolo Ruggeri, Fabio Peron, Marco Caniato, Andrea Gasparella</i>	77
Simulation of Thermal and Acoustic Façade Insulation Starting From the Characteristics of the Individual Elements <i>Nicola Granzotto, Paolo Ruggeri, Fabio Peron, Marco Caniato, Andrea Gasparella</i>	85
Climate Change Impact on Historical Buildings: A Case Study Within the Interreg Ita-Slo Secap Project <i>Marco Manzan, Amedeo Pezzi</i>	95
Hourly Dynamic Calculation of the Primary Energy With Heat Pump Generation System (EN 15316-4-2): A Case Study in Italy <i>Giada Remia, Serena Summa, Luca Tarabelli, Costanzo Di Perna</i>	103
A Project Focused on Sound Diffusion: The Acoustics of the Auditorium Yves St Laurent of Marrakech in Combination With its Innovative Architectural Design <i>Lamberto Tronchin, Antonella Bevilacqua, Ruoran Yan</i>	111
On the Prints of Another Horseshoe-Shaped Historical Building: Acoustic Studies of the Bonci Theatre of Cesena <i>Antonella Bevilacqua, Ruoran Yan</i>	117
Acoustic Discoveries of Another Masterpiece by Antonio Galli Bibiena: The Communal Theatre of Bologna <i>Antonella Bevilacqua, Ruoran Yan</i>	123
In Situ Measurement of Wall Thermal Properties: Parametric Investigation of the Heat Flow Methods Through Virtual Experiments Data <i>Andrea Alongi, Luca Sala, Adriana Angelotti, Livio Mazzarella</i>	129

Investigating the Performance of Different Window Opening Styles for Single-Sided Wind-Driven Natural Ventilation Using CFD Simulations <i>Akshit Gupta, Annamaria Belleri, Francesco Babich</i>	137
The Management of the Energy Performance Simulation of a Complex Building Portfolio. The Case of the School Building Asset of an Italian Municipality <i>Claudia Bo, Enrico De Angelis, Andrea Augello</i>	145
Hourly-Simplified Calculation to Identify Cost-Optimal Energy Performance Requirements for the Italian Building Stock <i>Matteo Piro, Franz Bianco Mauthe Degerfeld, Giovanna De Luca, Ilaria Ballarini, Vincenzo Corrado</i>	153
A Novel Methodology for Risk Assessment of Airborne Transmission due to Covid-19 in University Classrooms <i>Giulia Lambertini, Roberto Rugani, Fabio Fantozzi</i>	161
Integrated Approach to Assess the Energy and Environmental Payback Time of Buildings Refurbishment: A Case Study <i>Marta Roncone, Francesco Asdrubali, Gianluca Grazieschi, Chiara Tonelli</i>	169
Comparison Between Measured and Calculated Values in Relation to Noise From Wind Turbines <i>Antonella Bevilacqua, Gino Iannace, Ilaria Lombardi, Amelia Trematerra</i>	177
Thermo-Hygrometric Comfort Analysis in a Real Public Conference Room to Support a Digital-Twin Targeted to Parametric Investigations <i>Roberto Bruno, Piero Bevilacqua, Daniela Cirone, Natale Arcuri</i>	185
Validation of Energy Simulations of a Sustainable Wooden House in a Mediterranean Climate <i>Piero Bevilacqua, Roberto Bruno, Daniela Cirone, Stefania Perrella, Natalia Shushunova, Natale Arcuri</i>	193
Thermal and Acoustic Simulation of a Technical Enclosure for High Voltage Control Equipment <i>Edoardo A. Piana, Somayan Basu, Francesco Palone, Simone Sacco, Roberto Spezie</i>	199
Investigating the Role of Humidity on Indoor Wellness in Vernacular and Conventional Building Typologies <i>Suchi Priyadarshani, Roshan R Rao, Monto Mani, Daniel Maskell</i>	207
An Investigation Into Thermal Performance of Buildings Built Using Upcycled End-Of-Life Photovoltaic Panels <i>Roshan R Rao, Suchi Priyadarshani, Monto Mani</i>	217
Determining the Energy Benefits from Passive Solar Design Integration through the Sensitivity Analysis of Different Case Studies <i>Giacomo Cillari, Alessandro Franco, Fabio Fantozzi</i>	225
A Novel Personal Comfort System: A Radiant Desk With a Loop Heat Pipe <i>Roberto Rugani, Marco Bernagozzi, Marco Picco, Giacomo Salvadori, Fabio Fantozzi</i>	233
Energy Signature Modeling Towards Digital Twins – Lessons Learned From a Case Study With TRV and GAHP Technologies <i>Massimiliano Manfren, Maria Cristina Tommasino, Lamberto Tronchin</i>	243
The Amintore Galli Theatre in Rimini: A Dataset of Building Simulation Tools for its Acoustic Design <i>Antonella Bevilacqua, Massimiliano Manfren, Maria Cristina Tommasino, Ruoran Yan, Lamberto Tronchin</i>	249
Data-Driven Building Energy Modelling – Generalisation Potential of Energy Signatures Through Interpretable Machine Learning <i>Massimiliano Manfren, Maria Cristina Tommasino, Lamberto Tronchin</i>	255
Estimated Versus Actual Heating Energy Use of Residential Buildings <i>Matthias Schuss, Martin Fleischhacker, Ardeshir Mahdavi</i>	265
Polyamide Waste Thermal and Acoustic Properties: Experimental and Numerical Investigation on Possible Reuse for Indoor Comfort Improvement <i>Manuela Neri, Eva Cuerva, Alfredo Zabaleta, Pablo Pujadas, Elisa Levi, Ondrej Sikula</i>	273
Assessment of Demand-Side Management on the Performance of a Single-Dwelling Mechanical Ventilation Plus Radiant Floor System <i>Paolo Bonato, Anton Soppelsa, Marta Avantaggiato, Roberto Fedrizzi</i>	281
Passive Design Strategies for the Improvement of Summer Indoor Comfort Conditions in Lightweight Steel-Framed Buildings <i>Nicola Callegaro, Max Wieser, Giovanni Manzini, Ivan Kharlamov, Rossano Albatici</i>	289
Energetic Optimisation of the Domestic Hot Water System in a Residential Building by Means of Dynamic Simulations <i>Paolo Valdiserri, Aminhossein Jahanbin, Giovanni Semprini</i>	299

Assessing the Climate Resilience of Passive Cooling Solutions for Italian Residential Buildings <i>Mamak P. Tootkaboni, Ilaria Ballarini, Vincenzo Corrado</i>	305
Ventilation of Residential Buildings in Alpine Region: A Comparison Between Natural, Mechanical, and Mixed-Mode Strategies <i>Francesca Avella, Paolo Bonato, Annamaria Belleri, Francesco Babich</i>	313
A Comparison Among Three Whole-Building Dynamic Simulation Software and their Applicability to the Indoor Climate Modelling of Historical Buildings <i>Francesca Frasca, Elena Verticchio, Michele Libralato, Paola D'Agaro, Giovanni Cortella, Anna Maria Siani, Cristina Cornaro</i>	321
QGIS-Based Tools to Evaluate Air Flow Rate by Natural Ventilation in Buildings at Urban Scale <i>Silvia Santantonio, Guglielmina Mutani</i>	331
Modeling Energy Consumption in a Single-Family House in South Tyrol: Comparison Between Hemp Concrete and Clay Bricks <i>Silvia Ricciuti, Irene Lara-Ibeas, Annamaria Belleri, Francesco Babich</i>	341
A Fully Automated and Scalable Approach for Indoor Temperature Forecasting in Buildings Using Artificial Neural Networks <i>Jakob Bjørnskov, Muhyiddine Jradi, Christian Veje</i>	349
Effects of Different Moisture Sorption Curves on Hygrothermal Simulations of Timber Buildings <i>Michele Libralato, Maja Danovska, Giovanni Pernigotto, Andrea Gasparella, Paolo Baggio, Paola D'Agaro, Giovanni Cortella</i>	357
Energy Performance Evaluation and Economical Analysis by Means of Simulation Activities for a Renovated Building Reaching Different Nzeb Definitions Targets <i>Riccardo Gazzin, Jennifer Adami, Mattia Dallapiccola, Davide Brandolini, Miren Juaristi Gutierrez, Diego Tamburrini, Paolo Bonato, Martino Gubert, Stefano Avesani</i>	367
Preliminary CFD Parametric Simulations of Low- and Medium-Density Urban Layouts <i>Ritesh Wankhade, Giovanni Pernigotto, Michele Larcher</i>	377
Smart Sensors and Auditory Sensitivity: Acoustic Optimization of Dedicated Spaces for Autistic Individuals <i>Federica Bettarello, Marco Caniato, Arianna Marzi, Giuseppina Scavuzzo, Andrea Gasparella</i>	387
Simulation Application for the Assessment of the Energy Performance of a Building Renovated Using I-BEST System (Innovative Building Envelope through Smart Technology) <i>Cristina Carpino, Mario Maiolo, Patrizia Piro, Roberto Bruno, Natale Arcuri</i>	395
Modeling Occupants' Behavior to Improve the Building Performance Simulation of Classrooms <i>Federica Morandi, Julian Donges, Ilaria Pittana, Alessandro Prada, Francesca Cappelletti, Andrea Gasparella</i>	403
Modeling and Measurements in Natural Ventilation of Massive Buildings: A Case Study <i>Francesco Asdrubali, Luca Evangelisti, Claudia Guattari, Marta Roncone, Lucia Fontana, Ginevra Salerno, Chiara Tonelli, Valeria Vitale</i>	411
Calibration of the Energy Simulation Model of a Library with a Meta-Model-Based Optimization Approach <i>Maja Danovska, Alessandro Prada, Paolo Baggio</i>	417
Development of a Detailed Model of Hybrid System Composed by Air-to-Water Heat Pump and Boiler <i>Erica Roccatello, Alessandro Prada, Marco Baratieri, Paolo Baggio</i>	427
The Role of Ventilation in Indoor Spaces During the Covid-19 Pandemic: Comprehensive Analysis of ASHRAE Standard 62.1 <i>Giovanni Francesco Giuzio, Giovanni Barone, Annamaria Buonomano, Gianluca Del Papa, Cesare Forzano, Adolfo Palombo, Giuseppe Russo</i>	437
Design of Energy-Neutral Smart Buildings: An Ontological Framework to Integrate LCA, BIM and PLM <i>Tarun Kumar, Monto Mani</i>	449
Assessing the Performance of a Simplification Algorithm for Urban Building Energy Modeling in Multi-Objective Optimization <i>Federico Battini, Giovanni Pernigotto, Andrea Gasparella</i>	457
Application of a Simplification Algorithm for Urban Building Energy Modeling to Complex-Shaped Educational Buildings <i>Matteo Merli, Federico Battini, Giovanni Pernigotto, Andrea Gasparella</i>	465
Numerical Investigation of Radiation Efficiency of a Cross-Laminated Timber Floor <i>Marco Caniato, Nicola Granzotto, Federica Bettarello, Arianna Marzi, Paolo Bonfiglio, Andrea Gasparella</i>	473

Assessment of Contagion Risk due to Covid-19 for a Multi-Zone Building Model of Offices <i>Riccardo Albertin, Alessandro Pernici, Giovanni Pernigotto, Andrea Gasparella</i>	479
Impact of Visual, Thermal, and Indoor Air Quality Conditions on Students' Wellbeing and Learning Performance in a Primary School of Bolzano, Italy <i>Giovanni Demozzi, Luca Zaniboni, Giovanni Pernigotto, Andrea Gasparella</i>	489
Performance Simulation of Desiccant Wheel under Dynamic Conditions: <i>Comparison between Detailed and Simplified Models</i> <i>Simone Dugaria, Andrea Gasparella</i>	499
BIM and Mixed Reality for Visualizing Building Energy Data <i>Dietmar Siegele, Paola Penna, Iaria Di Blasio, Michael Riedl</i>	507
Impact of Solar Radiation Modelling on the Simulated Building Energy Performance in the Climate of Bolzano, Italy <i>Giovanni Pernigotto, Alessandro Prada, Aleksandr Gevorgian, Andrea Gasparella</i>	515
Effect of the Time Interval Base on the Calculation of the Renewable Quota of Building in an Alpine Context <i>Margherita Povolato, Alessandro Prada, Paolo Baggio</i>	525
Innovative Approaches for Teaching BPS: First Implementations of Business Game-Like Activities <i>Andrea Gasparella</i>	533

Preface

The participation of about 100 attendees at the fifth Building Simulation Applications BSA2022 Conference, one of the first IBPSA conferences held entirely in presence after the pandemic outbreak, can certainly be claimed as a step forward in the process of overcoming the constraints and limitations imposed by the years of the Covid-19 pandemic.

11 conference sessions in two parallel tracks, 66 presentations reporting the contributions by more than 180 authors are some of the most significant figures of this event. In addition, confirming an international profile and its inclusivity call, the Conference saw a small but significant presence of delegates from abroad, especially from Austria and India.

As the previous editions, BSA 2022 focused on providing an overview of the latest applications of building simulation in the following three main fields: the use of simulation for building physics applications, such as building envelope and HVAC system modelling and their design and operation optimization; global performance and multi-domain simulations; the development through simulation of new methodologies, regulations, as well as new calculation and simulation tools.

Nonetheless, the times urged to address indoor air quality, the main topic of this edition, emphasizing the role of simulation to assess strategies able to ensure healthy and safe indoor conditions for occupants.

The engaging opening speech about “The Role of IBPSA and Post-Covid Simulation” by Prof. Lori McElroy, President of IBPSA, was followed by two innovative and capturing keynotes, “Simulation and Optimization: Supporting Building Decarbonization” by Prof. Paolo Baggio, University of Trento, Italy, and “Going Digital – Infrastructure Modeling for Resilience and Decarbonization”, by Dr. Drury B. Crawley, vice-President of IBPSA.

The conference also devoted some time to the analysis and discussion of the use of building simulation among building professionals and specialists in terms of education: The “3rd Student School on Building Performance Simulation Applications” addressed the use of building performance simula-

tion in the context of building rating systems and in relation with BIM. We also had an interesting conversation with Lori McElroy on the topic of “Building Simulation in the Profession: Work in Progress”, discussing the current most critical aspects and challenges. Finally, after the conference closing ceremony on the third day, the “Round Table for Designers and Practitioners” featured four professional experiences about the use of building simulation, with a discussion about errors, challenges, and opportunities.

The fifth edition of the BSA conference represented an opportunity to restart and revitalize the process of reducing the gaps between academia and the professional world, of rethinking the role of building simulation in the design practice for future buildings, and of opening in the face of unprecedented challenges and opportunities of a new post-pandemic society.

Andrea Gasparella, Free University of Bozen-Bolzano

QGIS-Based Tools to Evaluate Air Flow Rate by Natural Ventilation in Buildings at Urban Scale

Silvia Santantonio – Politecnico di Torino, Italy – silvia.santantonio@polito.it

Guglielmina Mutani – Politecnico di Torino, Italy – guglielmina.mutani@polito.it

Abstract

Urban-scale evaluations of aerodynamic and morphological parameters allow correction of the wind speed within the urban boundary layer, as the wind profile is strongly influenced by the presence of roughness elements. This can have important implications for defining urban strategies for the reduction of buildings' energy consumption and the improvement of air quality and liveability of outdoor spaces. Among the current models for assessing the air flow rate by natural ventilation in buildings at urban scale, this study aims to define a GIS-based methodology, using existing databases and an open source QGIS plug-in. From a digital surface elevation dataset, and considering prevalent wind directions, the displacement height (z_a) was determined. The wind speed was corrected, applying the logarithmic or turbulent laws of wind profile, respectively, above and below z_a . This method could determine the spatial distribution of wind speed, considering each building façade characteristics and its surroundings. Resulting wind pressure on windward and leeward façades drives the air flow rate inside the buildings. Further developments of this work will improve the air flow modelling in buildings with other tools for applications at urban scale.

1. Introduction

Understanding and modeling the urban local wind environment has been a focus of attention for many researchers, especially in high density urban areas. Here, the heterogeneity of urban morphology, due to the presence of different type of roughness elements, strongly influences local wind performance (Peng et al., 2019). Studying air flow properties has important implications for urban design in terms of energy consumption, outdoor thermal comfort, and air quality, and building energy performance for

space heating and cooling (Suszanowicz, 2018). Relations between urban morphology and wind flow can be assessed with different methods: i) field measurements, whose high time and cost limitations mean that they are not suitable for large scale studies; ii) wind tunnel experiments, which constitute the reference dataset, despite operating costs and application limits; iii), Computational Fluid Dynamic (CFD) numerical modellings with high computational requirements (Buccolieri & Hang, 2019); iv) parametric models, mainly based on wind tunnel test or CFD simulations, having a good cost-benefit ratio but limited application field; v) Geographical Information System (GIS) and remote sensing techniques that retrieve roughness parameters based on interactions with buildings' geometries at city-scale, especially at mesoscale (Wong et al., 2010). Into the last group fits the place-based methodology presented in this work: a flexible integration of physical laws of wind phenomena and local characteristics of the urban context, based on the open-source software QGIS and existing databases, already used by urban planners. The study is part of broader research that aims to implement an hourly GIS-based engineering model to assess the energy consumption for the space heating and cooling of residential buildings at urban and district scales (Mutani & Todeschi, 2020; Mutani et al., 2022). The implementation concerns the monthly and hourly detail definition of number of air change per hour (ach) that influences thermal loads by natural ventilation in the building's thermal energy balance, considering the air flow rate for infiltration caused by wind-driven effects. The wind pressure generated on a building façade is evaluated as a function of the vertical and horizontal distribution of wind speed, starting from the characterization of roughness and

built environment characteristics. After a brief description of natural wind profiles in urban areas, this work aims to present some QGIS tools currently available to assess the urban wind field and its relationship with roughness parameters, applying the methodology to a case study.

2. Physical Laws of Wind Profiles

The wind phenomenon is influenced by the surface roughness of the ground and other objects (i.e., buildings, vegetation) that create obstacles to the undisturbed flow. A wind profile is associated with different environmental contexts (i.e., urban, sub-urban, rural areas), describing mathematically the mean wind speed (U_z) as a function of height (z) from the ground. Reference heights individuate boundary layers that limit air flow zones in which different physical laws can be applied.

2.1 Boundary Layers and Heights

In this work, reference was made to an older bibliography for defining wind phenomena, and to a more recent one for applying physical laws. Considering the horizontal scale of wind influence, three scale of interest exist (Oke, 2004): i) the *mesoscale*, where weather and climate are influenced by the whole city; ii) the *local scale*, where landscape features or topography are considered; iii) the *microscale*, where variations occur over very short distances, causing great airflow perturbations around roughness elements. Regarding the vertical scale of wind influence, relevant boundary layers and heights are defined:

- Atmospheric Boundary Layer (ABL)

In the ABL, or Planetary Boundary Layer, which extends up to 1-2 km (Z_{ABL} in Fig.1), the undisturbed wind flow present in upper layers is progressively slowed down due to friction with the ground and roughness elements. In the case of smooth soils (i.e., rural areas) the wind speed reaches upper layers values more quickly than urban areas.

- Urban Boundary Layer (UBL)

The UBL identifies the part of the ABL influenced by the presence of a large city. It is divided into:

Mixed Layer (ML), whose upper limits coincide with the height of UBL (Z_i , in Fig.1), and Surface Layer (SL) whose depth is about a tenth of UBL ($Z_{i/10}$, in Fig.1), and which, in turn, is divided into two.

- Internal Sub-Layer (ISL)

In the upper layer of SL, the flow is free of individual wakes associated with roughness elements, and wind can be assumed as a constant flux with a laminar, horizontally homogeneous flow ($Re < 2000$). Here, the wind log law can be applied to determine average wind speed (U_z).

- Roughness Sub-Layer (RSL)

This extends from ground level to the blending height Z_{RSL} (Fig. 1), where effects of individual roughness elements are visible. Airflow perturbation caused by individual surface and obstacles persists for a certain distance until it is mixed with the effect of turbulent eddies. Blending distance depends on the magnitude of the effect, the wind velocity, and the stability of the flux. Minimum $Z_{RSL} = 2 \cdot Z_H$ is suggested by observations in dense urban settings (Oke, 2004); it can vary with density, staggering, and heights of objects.

- Urban Canopy Layer (UCL)

This is equivalent to the mean height Z_H (Fig. 1) of the main roughness elements. To overcome the frictional effect of surface roughness elements, the wind flux loses its momentum: turbulent flows are generated near the surfaces ($Re > 4000$). Lower wind speed can occur, and turbulent models are required to calculate wind velocity inside urban canyons.

2.2 Aerodynamic Roughness Parameters

At local and micro scale, in the air zone where the flow is free from roughness-element turbulent wakes, two aerodynamic parameters are used to describe the wind speed profile influenced by surface roughness elements (Fig. 1):

- Zero-plane displacement height (z_d)

It is intended as a new "ground level" from which the wind profile originates, after the wind passes over high-density buildings (Lv et al., 2022), and it is used for setting a base for the application of the wind log law (Oke, 2004). According to (Abubaker et al., 2018), it is the depth of still air trapped among the roughness elements.

- Roughness length (z_0)

This is the height above Z_d at which wind velocity becomes zero when the logarithmic wind profile is applied and represents the size of the eddies produced from wind moving over a rough surface (Abubaker et al., 2018). It depends on turbulence intensity and, therefore, on the surface drag.

In urban areas, three flow regimes were classified when aerodynamic parameters are morphometrically determined (Oke, 2004): i) *isolated flow*, where buildings are individual wake generators; ii) *wake interference flow*, where wakes reinforce each other as space between buildings is close; iii) *skimming flow*, where main flow skips over the top of the great density of buildings. The wake interference regime is the one in which the greatest roughness activity can be generated. The building density (λ_p) is very important in cities, where the high variability of roughness height can cause complex surface morphology and turbulent wakes that are challenging to assess.

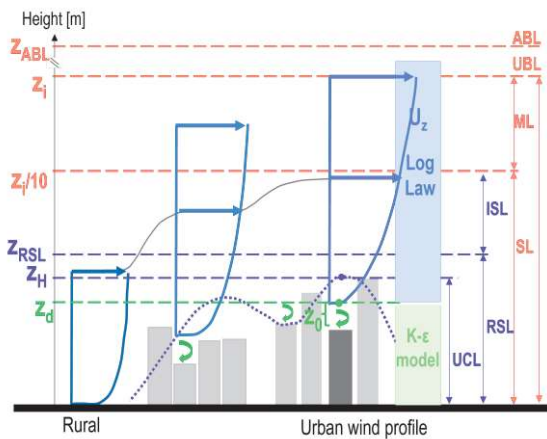


Fig. 1 – Boundary layers and their reference height (y axis) at mesoscale (in orange) and local scale (in purple)

2.3 Wind Profiles Laws at District Scale

In this work, two methods were compared to determine the wind speed (U_z), from measured U_{ref} at reference height (z_{ref}): the *C_p methodology* and *z_d methodology*, whose procedures are schematized in Fig. 2. U_{ref} need to be adjusted considering the wind incident angle (Eq. 1, in Fig. 2) and objects and terrain roughness of the context. For wind fluxes that occur above the displacement height z_d , two wind profiles can be applied.

The power law wind profile is based on empirical assumption for mesoscale application for large heights ($30 \text{ m} < z < 300 \text{ m}$), but it is less accurate when close to the ground. It can be determined according to Eq. 2 (Fig. 2), where V_z is the wind speed at height z [m·s⁻¹], $U_{ref,corr}$ is the adjusted reference wind speed [m·s⁻¹] at height z_{ref} , Z_{UBL} is the height of the UBL [m], and v the terrain roughness coefficient (wind speed profile exponent) [-]. The last two parameters refer to tabular data, determined through empirical assumptions from real measurements or wind tunnel tests. Several references exist in the literature, including the unified terrain roughness categories given by (Choi, 2009). Table 1 reports typical values for roughness parameters for the most used terrain categories.

Table 1 – Referenced roughness parameters for terrain typology

Terrain roughness type	Z_{UBL} [m]	v [-]	Z_0 [m]	Z_d [m]
Level surfaces, grass land	250	0.10	-	-
Flat open country	280	0.14	0.03	0.0
Rolling/level surfaces	300	0.22	0.1	0.0
Heterogeneous surface	330	0.28	-	-
Low density suburban areas	390	0.34	0.5	$0.7 \cdot Z_H$
Mid-high density urban areas	450	0.40	1.0	$0.8 \cdot Z_H$
Very high density city areas	510	0.45	> 2.0	$0.8 \cdot Z_H$

The logarithmic law wind profile allows an approximation of the wind profile at lower boundary condition ($z \leq 200\text{m}$). Its lower limit of application at urban local scale is identified by z_0 and z_d , according to the logarithmic function of Eq. 3 (Fig. 2), where U_z is the wind speed [m·s⁻¹] at height z , $U_{ref,corr}$ is the corrected wind speed at height z_{ref} , z_d is the zero-plane displacement height [m], and z_0 is the roughness length [m]. At microscale, inside the urban canopy layer, where turbulent fluxes occur at a height z lower than displacement height z_d , the log-law is not valid and turbulent models should be applied. The k-epsilon (k-ε) model is the most common model in CFD analyses for simulating the mean flow characteristics for turbulent flow conditions. It belongs to the Reynolds-averaged Navier Stokes (RANS) models that represent an optimal compromise between accuracy and efficiency for microclimate studies in urban environments (Janroodi et al., 2022).

2.4 Wind Flow at Building Local Scale

Natural ventilation in buildings is driven by pressure differences on building façades by two forces: the stack (or buoyancy) effect and the wind-driven effect. This work focuses on the latter, while in future works, buoyancy will be considered in a multi-zones airflow model to assess ventilation loads in buildings. Wind generates positive pressure and negative pressure on windward and leeward façades, respectively. The surface pressure (P_s, P_v) can be calculated according to Eq.4 or Eq.5 (Fig. 2), respectively, with C_p and z_d methodology, where ρ is air density [$\text{kg}\cdot\text{m}^{-3}$], V_z (power law) and U_z (log-law) are the adjusted wind speed [$\text{m}\cdot\text{s}^{-1}$] and C_p is the pressure coefficient [-]. It is a non-dimensional coefficient estimated according to i) real scale measurements, ii) wind tunnel tests, iii) CFD and iv) parametric models, among which there is *Cpcalc+* software (Chiesa & Grosso, 2019), whose input data are listed in Table 2. Even if the power law application determines a vertical variation of wind velocity at the local urban scale, the C_p allows the distribution of wind speed horizontally and vertically at the scale of interesting points on a building façade with respect to the windward and leeward façade dimensions; it also considers building geometry and orientation, urban density, and roughness characteristic of the surrounding environment. The algorithm used in *Cpcalc+* is based on experimental wind tunnel tests results, considering different typical buildings and urban contexts (e.g., Fracastoro et al., 2001). Limitations of the software concern the scale of the application field (suitable at building scale, not at district-urban scale), and the application range of some parameters, especially the relative building height and the aspect ratios ($0.5 \leq \text{FAR} \leq 4$ and $0.5 \leq \text{SAR} \leq 2$).

Table 2 – Input data required by *Cpcalc+* software (<https://iris.polito.it/handle/11583/2579969>)

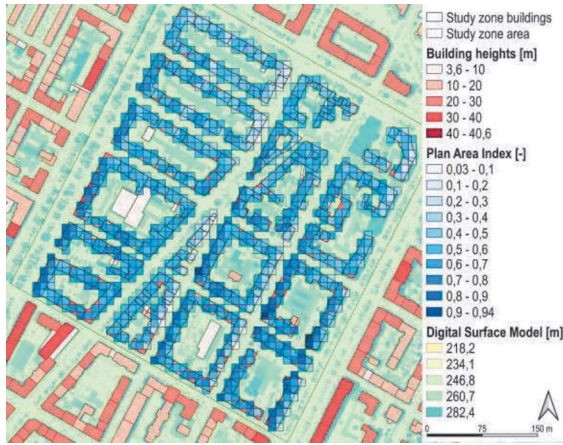
Climate data			
Wind speed		Wind direction	
Urban parameter			
Plan Area Density	Surroundings building height	Wind profile exponent	
Building Characteristic			
Frontal/Side Aspect Ratio (FAR/SAR)	Building dimension	Building azimuth	Roof slope

2.5 Place-Based Tools and Plug-Ins for Wind Analysis at Urban Scale

In this paragraph, GIS-based tools and a plug-in to assess wind at urban scale are described.

SAGA GIS software presents some useful tools for wind correction at the mesoscale, to consider terrain influence on observed meteorological conditions. In the *Climate and Weather* section, the *Wind Effect Correction* tool allows the scaling factor of the wind effect in determining ABL conditions (e.g., precipitation, cloudiness) to be calibrated. In the *Terrain analysis - Morphometry* section, the *Wind Effect* tool classifies wind exposed and shades area through a dimensionless index, considering terrain elevation and specifying wind data; these tools were created for topo-climatic wind assessments. Existing methods to determine the aerodynamic parameters at urban scale can be grouped into three main classes: i) *reference-based values from field observations*, which provide a wide range of values whose application in complex and heterogenous urban areas has some limitations; ii) *anemometric methods* requiring experimental campaigns, applicable on a limited and non-replicable scale; iii) *morphometric methods* based on the relationships between aerodynamic parameters and roughness elements geometry, described through urban morphological parameters, already used both at mesoscale (Darmanto et al., 2017) and local scale (Badach et al., 2020). This work aims to present z_d methodology (Fig. 2), determining z_d and z_0 using the open-source QGIS plug-in Urban Multi-scale Environmental Predictor (UMEP), version 1.6.1 (Lindberg et al. 2016). Among the pre-processing tools, there are the *Urban Morphology- Morphometric Calculator (Grid)* and *(Point)*, which only differ in the geometry of the calculation area. Both calculate five morphometric parameters (Table 3, Fig. 3) based on digital surface models (DSM) to calculate the two aerodynamic parameters according to six different methods (Table 4). The required input data are three separate raster files (*geoTIFF*) with the same pixel resolution: DSM, digital elevation model (DEM, only ground elevation), and roughness elements elevation, calculated with the QGIS *Raster calculator tool*, by subtracting the other two rasters (DSM-DEM).

	Cp method	z_d method
Software:	CpCalc+	QGIS UMEP plug-in
Input data:	Wind speed (U_{ref}) from a reference height (z_{ref}) of the weather station	
Uref adjustment – wind incident angle (θ)	Eq. 1) $U_{ref,corr} = U_{ref} \cdot \cos(\theta)$ } θ wind incident angle normal to the windward building facade	
Uref adjustment – terrain and object roughness correction:	Power law wind profile Eq. 2) $V_z = U_{ref,corr} \cdot \left(\frac{z_{UBL,ref}}{z_{ref}}\right)^{V_z} \cdot \left(\frac{z}{z_{UBL,z}}\right)^{V_z}$ } Tabular data } Mesoscale vertical distribution for each z_n	Log law wind profile Eq. 3) $U_z = U_{ref,corr} \cdot \left[\frac{\ln\left(\frac{z-z_d}{z_0}\right)}{\ln\left(\frac{z_{ref}-z_d}{z_0}\right)}\right] \cdot \left[\frac{z_d}{z_0}\right]$ } GIS plug-in } Local scale vertical distribution for each z_n
		Turbulent wind profile } Uz from correlations of CFD results horizontal distribution for each grid cell
Pressure coefficient (Cp) calculation:	vertical and horizontal distribution on building facades (from CpCalc+)	
Surface pressure:	Eq. 4) $P_s [Pa] = \frac{1}{2} \cdot \rho \cdot V_z^2 \cdot C_p$	Eq. 5) $P_v [Pa] = \frac{1}{2} \cdot \rho \cdot U_z^2$
Limits of the methodology:	<ul style="list-style-type: none"> • Roughness correction at mesoscale (wide scale) • Roughness correction from tabular data (wide range values) • Application range of some parameters based on experimental tests ($0,5 \leq FAR \leq 4$ and $0,5 \leq SAR \leq 2$, building height) • Building scale application not suitable for district scale 	<ul style="list-style-type: none"> • Results accuracy strongly affected by the radius of calculation area and size of grid cells (no unified standard for selecting area) • Horizontal distribution of wind speed variation only for heights greater than Z_d (above canopy layer)

 Fig. 2 – Comparison between the Cp and z_d methodologies for the assessment of surface pressure generated by the wind flow

 Fig. 3 – Plan area index (λ_p) within its range (0-1) for a squared cell grid, considering building heights in a selected area

The main setting concerns the extension of the calculation area that will be considered to determine the morphological and aerodynamic parameters, indicating the radius length from the selected point or the centroid of each grid cell. There are no unified standards for the size of calculation area, though it greatly affects the accuracy of results (Lv et al., 2022). In addition, it is possible to specify the wind direction (in degrees, from north - clockwise). The five morphometric parameters calculated in UMEP correspond to some of the most frequently used urban parameters in the urban planning research field; Table 3 reports their definitions. The morphological and aerodynamic parameters can vary according to the analyzed wind direction, allowing more precise results of z_d and z_0 , considering the variability of the roughness surfaces (Oke, 2004).

Table 3 – Urban parameters defined in QGIS-UMEP tool

Urban parameter	Unit	Formula
Plan Area Index	[-]	$\lambda_p = (\sum_{i=1}^n A p_i) / A_T$
Frontal Area Index	[-]	$\lambda_f = (\sum_{i=1}^n A f_i) / A_T$
Mean Height	[m]	$z_H = (\sum_{i=1}^n H_i) / n$
Maximum Height	[m]	$z_{Hmax} = \text{Max}(H_i)$
Height variability	[m]	$z_{Hstd} = \sqrt{\frac{1}{n} \sum_{i=1}^n (H_i - z_H)^2}$

The UMEP tool calculates the aerodynamic roughness parameters (z_d , z_0) by applying six different morphometric methods (Kent et al., 2017). For each method, Table 4 reports urban parameters used in the calculation: plan area density (λ_p), frontal area ratio (λ_f), average (z_H) and maximum (z_{Hmax}) buildings height and height variability (z_{Hstd}). In this work, the Kanda method was used (Kanda et al., 2013), as it is more suitable in dense, city-center districts, due to the importance of considering roughness elements' height heterogeneity. The flow chart in Fig. 4 summarizes the z_d methodology used to determine the aerodynamic parameters and the proper wind profile with the QGIS UMEP plug-in.

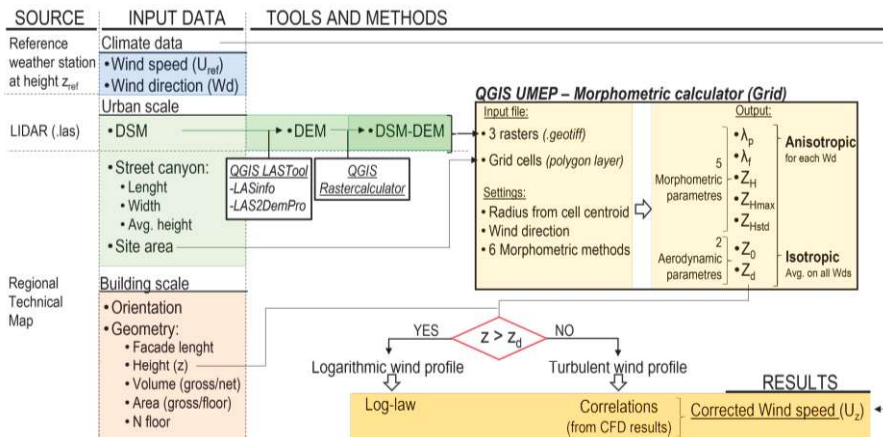


Fig.4 – Flow chart of the z_d methodology based on QGIS-UMEP tools

Table 4 – Morphometric methods included in the UMEP plug-in

Method	Urban Parameter				
	λ_p	λ_f	Z_H	Z_{Hmax}	Z_{Hstd}
Rule of thumb			X		
Raupach		X	X		
Bottema	X	X	X		
Macdonald	X	X	X		
Millward-Hopkins	X	X	X		X
Kanda	X	X	X	X	X

3. Application of the UMEP Tool at District Scale in Turin

The place-based methodology was applied to a central district in the city of Turin (Italy). For an in-depth analysis of case study zone (200 m x 200 m) selection criteria and characteristics, refer to (Mutani et al., 2021). The local monthly prevalent wind is from North-NorthEast and West-SouthWest, with a mean velocity of 1.4 m/s. Table 5 shows main the urban parameters calculated in QGIS to describe the case study area.

Table 5 – Morphological and roughness characteristic of the area

Urban parameter	Unit	Study area
Built Coverage Ratio (BCR)	[-]	0.33
Plan Area Density (PAD)	[-]	1.66
Volume Area Ratio (VAR)	[-]	0.30
Surrounding buildings' height	[m]	19.5
Height of boundary layer (z_{UBL})	[m]	450
Wind speed profile exponent (ν)	[-]	0.4
Short urban canyon (L/H)	[m]	≤ 3
Long urban canyon (L/H)	[m]	> 5

For the UMEP tool application, a grid vector polygon was created, with a 5-m-squared grid, and results were assigned to grid cells and related buildings. Three raster files were created, starting from a 1-m resolution surface elevation dataset (DSM). From the centroid of each cell of the grid, a 300m radius study area was set, obtaining, for each cell, 12 different results of morphological and aerodynamic parameters, for 12 wind directions.

4. Results and Discussion

The UMEP tool results are the *anisotropic* and *isotropic* output: the first gives values for each wind direction, the second reports mean values of all wind directions. Fig. 5 shows the isotropic results of the displacement height z_d for the case study zone. The anisotropic results of z_d consider the two prevalent wind directions (N-NE, Fig.6a and W-SW, Fig.6b). Results were assessed at the building scale. According to building heights (z) and floor numbers, for each floor, the wind speed was adjusted applying the log law (if $z > z_d$) or the turbulent motion equation (if $z \leq z_d$). Buildings were classified into those with logarithmic and turbulent wind profile, or only turbulent profile (red and blue points, in Fig. 6a-b, respectively). Figs. 6a-6b show that the buildings for which the log law is valid are those located in urban canyons oriented parallel to the prevailing wind direction. In this work, the wind speed above z_d was calculated applying the log law equation (Eq.3, in Fig.2), while below z_d , it was calculated based on correlations

found from the CFD model results (Javanroodi et al., 2022). Reference was made to a case study with similar urban morphological characteristics (Table 5); linear and exponential correlations were determined for short and long canyons (Fig. 7).

A block of buildings (red rectangle, Fig. 6a) well exposed to the N-NE wind, was selected to assess the surface pressure generated by the wind on the windward façade of buildings, comparing results of the two different methodologies (Fig. 2). Wind speed was corrected applying the power law (C_p method) and log law (z_d method), at three representative heights for each building in the block (first floor- z_1 , average floor- z_2 , top floor- z_3) and 30 points on windward block façade (i.e., 1-30).

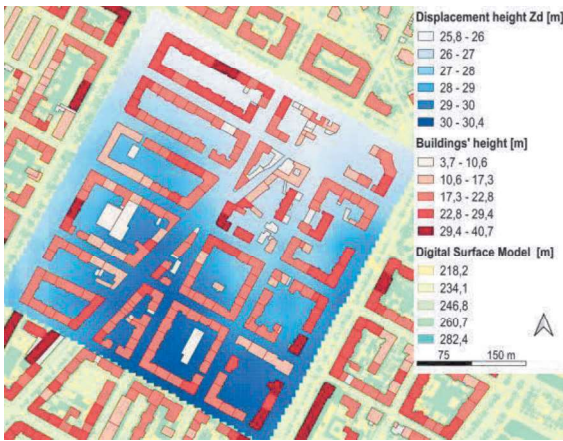


Fig. 5 – Isotropic result of the displacement height z_d [m].

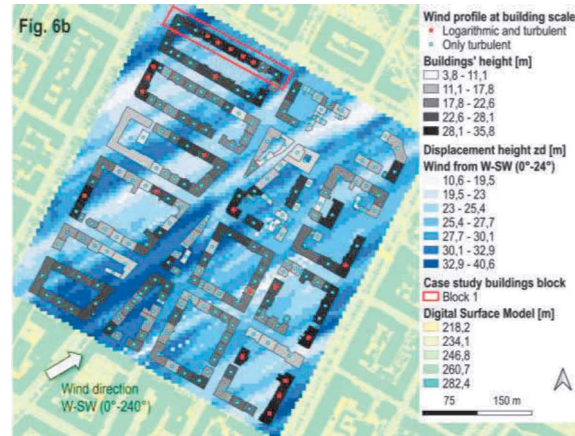


Fig. 6 a,b – Anisotropic result of displacement height z_d , for wind direction N-NE (a) and W-SW (b)

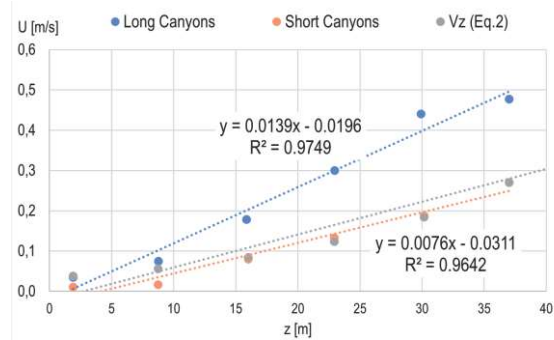


Fig. 7 – Correlations for long (blue) and short (orange) canyons

To horizontally distribute the wind speed along the windward façade, C_p was calculated with the C_{pcalc+} ; in the z_d method, a value of z_d and z_0 was determined for each cell of the grid, obtaining a different wind velocity for each cell spatially distributed in front of the façades. Considering the three heights of building, Fig. 8 shows results of the surface pressure P_s and P_v , calculated with C_p -method and z_d -method, respectively.

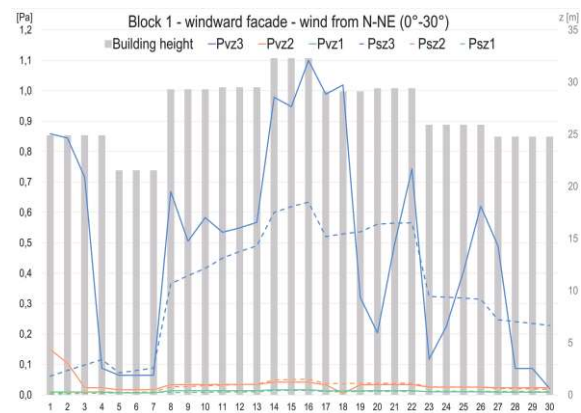


Fig. 8 – Surface pressure calculated with the c_p method (P_s , dotted lines) and the z_d method (P_v , continuous line)

It can be noticed that, for the height z_3 (blue line), above z_d , results of *z_d-method* are more precise than the *cp-method* one when describing variations that occur on façades and that are mainly due to the wind wakes generated from surrounding buildings. The main limit of the *cp-method* concerns its range of application, since the analyzed block exceeds the aspect ratio range ($FAR > 4$). For heights (z_1, z_2), below z_d , surface pressures are very low in both methods, due to the reduced wind speed inside the canyon (Fig. 8).

5. Conclusion and Further Development

This study aims to determine the variation in wind speed at local scale as a function of roughness elements and their effects on the urban context. The model's place-based approach, based on accessible databases and open-source software (QGIS), is applied at neighbourhood scale and it is adaptable to other contexts and urban scales. The methodology presented determines heights of boundary canopy layer (z_d, z_0) to apply the proper wind profile law, in relation to building heights. If compared to the *Cp method*, it can assess horizontal wind speed distribution along building façades, and to calculate surface pressure driving the air flow rate inside buildings. This aspect can be further investigated thanks to the flexibility of GIS place-based methodology. In fact, the novelty of this work lies in the possibility of adapting and integrating new or already existing software into QGIS, in the attempt to calculate the natural ventilation loads with a lumped model for all buildings at urban scale. A recent upgrade of the *CpCalc+* algorithm in a Python script (Chiesa & Grosso, 2019), constitutes an interesting opportunity for methodology implementation. Therefore, different scenarios can be investigated, including exploiting the GIS tool to retrieve all input data at urban scale necessary for *Cp* calculations, or directly integrating the *CpCalc+* algorithm into a dedicated QGIS plug-in. A simplified parametric model to evaluate wind flows around buildings at urban scale is essential for supporting urban planning in increasing buildings' energy performance and liveability of urban environments.

References

- Abubaker, A., I. Kostić, and O. Kostić. 2018. "Numerical modelling of velocity profile parameters of the atmospheric boundary layer simulated in wind tunnels". *IOP CS: Materials Science and Engineering* 393: 012025. doi: <https://doi.org/10.1088/1757-899X/393/1/012025>
- Badach, J., D. Voordeckers, L. Nyka, and M. Van Acker. 2020. "A framework for Air Quality Management Zones - Useful GIS-based tool for urban planning: Case studies in Antwerp and Gdańsk". *Building Environment* 174: 106743. doi: <https://doi.org/10.1016/j.buildenv.2020.106743>
- Buccolieri, R., and J. Hang. 2019. "Recent Advances in Urban Ventilation Assessment and Flow Modelling". *Atmosphere* 10(3). doi: <https://doi.org/10.3390/atmos10030144>
- Chiesa, G., and M. Grosso. 2019. "Python-based calculation tool of wind-pressure coefficients on building envelopes". *JPCS* 1343(1): 012132. doi: <https://doi.org/10.1088/1742-6596/1343/1/012132>
- Choi, E., 2009. "Proposal for Unified Terrain Categories Exposures Velocity Profiles". In 7th APCWE, Vol. VII.
- Darmanto, N. S., A. C. G. Varquez, and M. Kanda. 2017. "Urban roughness parameters estimation from globally available datasets for mesoscale modeling in megacities". *Urban Climate* 21: 243–261. doi: <https://doi.org/10.1016/j.uclim.2017.07.001>
- Fracastoro, G. V., G. Mutani, M. Perino. 2001. "A simple tool to assess the feasibility of hybrid ventilation systems". In 4th IAQVEC, Vol. III: 1421-1429, Hunan (China). ISBN:962-442-190-0
- Javanroodi, K., V. M. Nik, M. G. Giometto, and J.-L. Scartezzini, 2022. "Combining computational fluid dynamics and neural networks to characterize microclimate extremes: Learning the complex interactions between meso-climate and urban morphology". *STE* 829: 154223. doi: <https://doi.org/10.1016/j.scitotenv.2022.154223>
- Kanda, M., A. Inagaki, T. Miyamoto, M. Gryschka, and S. Raasch 2013. "A New Aerodynamic Parametrization for Real Urban Surfaces". *BLM* 148(2): 357–377. doi: <https://doi.org/10.1007/s10546-013-9818-x>
- Kent, C. W., et al., 2017. "Evaluation of Urban Local-Scale Aerodynamic Parameters: Implications for the Vertical Profile of Wind Speed and for Source Areas". *BLM* 164(2): 183–213. doi: <https://doi.org/10.1007/s10546-017-0248-z>
- Lindberg, F., et al., 2018. "Urban Multi-scale Environmental Predictor (UMEP): An integrated tool for city-based climate services". *Environmental Modelling & Software* 99: 70–87. doi: <https://doi.org/10.1016/j.envsoft.2017.09.020>
- Lv, G., et al., 2022. "An urban-scale method for building roofs available wind resource evaluation based on aerodynamic parameters of urban sublayer surfaces". *Sustainable Cities and Society* 80: 103790. doi: <https://doi.org/10.1016/j.scs.2022.103790>
- Mutani, G., and V. Todeschi. 2020. "Building energy modeling at neighborhood scale". *EE* 13 (7): 1353–1386. doi: <https://doi.org/10.1007/s12053-020-09882-4>
- Mutani, G., S. Santantonio, and V. Todeschi, 2021. "Evaluation of ventilation loads in buildings energy modelling at urban scale". In 2021 IEEE 4th CANDO-EPE 37–42. doi: <https://doi.org/10.1109/CANDO-EPE54223.2021.9667547>
- Mutani, G., S. Santantonio, and V. Todeschi, 2022. "Urban-Scale energy models: the relationship between cooling energy demand and urban form". *JPCS 38th UIT*, 2021, Gaeta (Italy).
- Oke. T. 2004. "Initial guidance to obtain representative meteorological observations at urban sites. Instruments and observing methods". World Meteorological Organization/TD 1250-81
- Peng, Y., Z. Gao, R. Buccolieri, and W. Ding. 2019. "An Investigation of the Quantitative Correlation between Urban Morphology Parameters and Outdoor Ventilation Efficiency Indices". *Atmosphere* 10(1). doi: <https://doi.org/10.3390/atmos10010033>
- Suszanowicz, D. 2018. "Optimisation of Heat Loss through Ventilation for Residential Buildings". *Atmosphere* 9(3). doi: <https://doi.org/10.3390/atmos9030095>
- Wong, M., et al. 2010. "GIS techniques for mapping urban ventilation, using frontal area index and least cost path analysis". *IAPRSS* 38(2):586-591.